



Contents lists available at ScienceDirect

Journal of King Saud University – Science

journal homepage: [www.sciencedirect.com](http://www.sciencedirect.com)

# Evaluation of antioxidant, antimicrobial and antiproliferative activity of silver nanoparticles derived from *Galphimia glauca* leaf extract

Bidhayak Chakraborty<sup>a</sup>, Raju Suresh Kumar<sup>b,\*</sup>, Abdulrahman I. Almansour<sup>b</sup>, D. Kotresha<sup>c</sup>, Muthuraj Rudrappa<sup>a</sup>, Pallavi S.S.<sup>a</sup>, Halaswamy Hiremath<sup>a</sup>, Karthikeyan Perumal<sup>d</sup>, Sreenivasa Nayaka<sup>a,\*</sup>

<sup>a</sup> Department of Studies in Botany, Karnatak University, Dharwad 580003, Karnataka, India

<sup>b</sup> Department of Chemistry, College of Science, King Saud University, P.O. Box 2455, Riyadh 11451, Saudi Arabia

<sup>c</sup> Department of Studies in Botany, Davangere University, Shivagangotri, Davangere 577007, Karnataka, India

<sup>d</sup> Department of Chemistry and Biochemistry, The Ohio State University, 151 W. Woodruff Ave, Columbus, OH 43210, USA

## ARTICLE INFO

### Article history:

Received 30 August 2021

Revised 30 September 2021

Accepted 12 October 2021

Available online 23 October 2021

### Keywords:

*Galphimia glauca*

Green synthesis

Antioxidant

Antimicrobial

Anticancer

SK-HEP1 cell line

Silver nanoparticles

## ABSTRACT

**Objective:** The bio-synthesis of silver nanoparticles (AgNPs) is regarded as environment friendly and cost effective method compared to physical and chemical synthesis methods. Silver (Ag) is an important noble metal due to its tremendous use in research and medical fields throughout the world. This research work was aimed at green synthesis and characterizations of AgNPs from *G. glauca* leaf extract and evaluation of their bioactive potential.

**Methods:** In the current research work, synthesis of AgNPs from *G. glauca* aqueous leaf extracts was performed and was characterized by UV-Visible (UV-Vis.), Fourier transform infrared (FTIR), Atomic force microscopy (AFM), Scanning electron microscopy (SEM), Energy dispersive spectroscopy (EDS), High-resolution transmission electron microscopy (HR-TEM), X-ray diffraction (XRD), Thermo gravimetric analysis (TGA) and Zeta potential exploration. Later, antioxidant, antimicrobial activity was examined against various pathogenic organisms and anticancer activities of AgNPs were carried out against SK-HEP1 cell line.

**Results:** The first indication of synthesis of nanoparticles was the change in color from yellowish to brown. UV-Vis. band exhibited surface plasmon resonance (SPR) at 402 nm. FTIR analysis revealed the probable bio-molecules including alkanes, alkenes, aromatics, aromatic phosphates, imine or oxime, etc. subjected to reduction of silver ions to metallic silver. The AFM, SEM and TEM analysis reported the particles were spherical shaped, poly-dispersed, 17 to 40 nm in size. The zeta potential analysis expressed a peak at  $-32.0 \pm 0.5$  mV and suggested the particles with significant long term stability. The TGA analysis revealed the stability of AgNPs at high temperature (179 °C). The antioxidant assay of AgNPs unveiled an effective dose dependent increase in scavenging activity. Antimicrobial activity showed efficient inhibitory activity against *P. aeruginosa* and *C. glabrata*. Lastly, the AgNPs revealed a strong anticancer activity against SK-HEP1 liver cancer cell line with an IC<sub>50</sub> value of 19.12 µg/mL.

**Conclusions:** Therefore, it could be concluded that a substantial in-vivo investigations are needed for antioxidant, antibacterial and anticancer activities, so that it will be useful in medical field in future.

© 2021 The Author(s). Published by Elsevier B.V. on behalf of King Saud University. This is an open access article under the CC BY-NC-ND license (<http://creativecommons.org/licenses/by-nc-nd/4.0/>).

## 1. Introduction

Nanotechnology can be considered as one of the most committed technologies having applications in almost every fields of science. Nanotechnology predominantly focuses on synthesis, design and manufacturing of particles with size, structure and dimensions lesser than 100 nm. The nanoparticles synthesized using noble metals is receiving global attention mainly due to their successful solutions for the challenges in bio-medicinal, catalysis, agriculture and pharmaceutical activities (Singh et al., 2016).

\* Corresponding authors.

E-mail addresses: [sraju@ksu.edu.sa](mailto:sraju@ksu.edu.sa) (R.S. Kumar), [sreenivasankud@gmail.com](mailto:sreenivasankud@gmail.com) (S. Nayaka).

Peer review under responsibility of King Saud University.



<https://doi.org/10.1016/j.jksus.2021.101660>

1018-3647/© 2021 The Author(s). Published by Elsevier B.V. on behalf of King Saud University.

This is an open access article under the CC BY-NC-ND license (<http://creativecommons.org/licenses/by-nc-nd/4.0/>).

In the recent research field of nanotechnology, synthesis of nanomaterials and their characterization is blooming since past two decennials. The development of stable green methodology for synthesis of AgNPs is an important parameter of current research in nanotechnology (Ponarulselvam et al., 2012; Devanesan and AlSalhi 2021). There are an ample number of noble metals practiced for the synthesis of nanoparticles including silver, titanium, chromium, platinum, zinc, iron, gold, cobalt, aluminum, nickel, copper, palladium, etc. However, silver is one of the worthiest among commonly used metals for synthesis of nanoparticles. Silver is considered as stone of wealth due to its wide applications. Although this metal is highly valuable and preferable due to its properties like flexibility, softness, resilient, glistening, conductive, antimicrobial, size and shape dependent optical behavior and easily obtainable (Guzel and Erdal, 2018; Devanesan et al., 2021). The most common utilizations of AgNPs and silver are in the medical business industries. The AgNPs are used in creams and topical ointments to avoid the infections of burns and wounds, the devices and implants used in medical field are manufactured with silver-loaded polymers and products of consumers, which contain silver, for instance silver-embedded fabrics, colloidal silver gel, etc., are used in sporting equipments (Song and Kim, 2009).

The synthesis process of AgNPs is involved in physical, chemical and biological means. The physical and chemical methodologies have several disadvantages like raising surrounding environmental temperature, huge energy consumption, uses of expensive, toxic and inflammable chemicals, etc. which make them unfavorable for the synthesis of AgNPs (Abou El-Nour et al., 2010, Veerasamy et al., 2011). Compared with physical and chemical synthesis green synthesis has many advantages because it requires less chemicals, devoid of lengthy process and requirement of huge energy and less contaminants that avoid expensive purifications (Awwad et al., 2013).

Several biological existences, which can possibly be employed for nanoparticles synthesis, such as plants extract of leaves, flowers, roots, bark, latex, organisms include actinomycetes, fungi, bacteria, algae and bio-molecules like amino acids, vitamins, etc. (Gurunathan et al., 2014; Guzel and Erdal, 2018). The biological synthesis is the most preferred method because of availability of stabilizing agents and capping agents and in the form of proteins, enzymes, amino acids, intra and extra cellular metabolites. The plant derived phyto-chemicals, like polysaccharides, alkaloids, terpenoids, flavonoids, saponins, phenolics, tannins also assure reduction process of nanoparticles. Thus, the use of environmentally favorable substances minimizes use of dangerous chemicals and thereby makes it reliable, easy, eco-friendly and inexpensive method (Das et al., 2017; Guzel and Erdal, 2018; Zhang et al., 2016). The plant-derived nanostructures, such as crystalline and planar gold nanostructures, spherical AgNPs, spherical Indium Oxide nanoparticles and cuboidal palladium nanoparticles are biologically synthesized and all are non-toxic, stable and can be used for different purposes, such as water treatment, drug-delivery, biosensing, photocatalysis, etc. (Oza et al., 2020).

The plant *Galphimia glauca* (*G. glauca*) is a member of the family *Malpighiaceae*. The plant is a shrub and mostly distributed in dry environments (Anderson, 2007). The plant is being used for the treatment of asthma, malaria, diarrhea, allergies, etc, which is mostly due to the presence of tri-terpinoid phytochemical called galphimines. This plant is rich in many phytochemicals, like flavonoids, galic acids, terpenoids, phenolics, etc. (Cardoso-Taketa et al., 2008; Sharma et al., 2018). These phytochemicals have anticarcinogenic, anti-inflammatory, antioxidant properties as well as neuroprotective activity (Oza et al., 2020). Gupta and Jeevaratnam (2019), studied the antimicrobial and anticancer activity of methanolic extract of leaf and bark extract of this plant, which revealed a significant antibacterial activity against MRSA

strains. The anticancer assay showed a relative reduction in viability of lung cancer and colon cancer cells.

The liver cancer is one of the most common cancers and a major cause of cancer deaths in the world. Every year around 800,000 people are diagnosed and account 700,000 deaths for this cancer. A deep literature review suggested that there is no report on green synthesis of AgNPs from *G. glauca*. To the best of our knowledge, this is the first report on green synthesis of AgNPs from *G. glauca* leaf aqueous extract and evaluation of its anticancer activity on SK-HEP 1 cell line. Therefore, keeping this in mind, in the present work, a green synthesis method of AgNPs was conducted to evaluate its antimicrobial and anticancer activity against human liver adenocarcinoma-SK-HEP1 cell line.

## 2. Materials and methods

### 2.1. Collection of materials and chemicals

The fresh green leaves of *G. glauca* were gathered from the Botanical garden, Karnatak University, Dharwad. All chemicals were purchased from HiMedia laboratories, India. Bacterial strains, such as *Staphylococcus aureus* (MTCC6908), *Enterococcus faecalis* (MTCC6845), *Bacillus cereus* (MTCC1272), *Escherichia coli* (MTCC40), *Klebsiella pneumoniae* (MTCC4030), *Pseudomonas aeruginosa* (MTCC424) and fungal cultures like *Candida glabrata* (MTCC3019), *Candida albicans* (MTCC227), *Magnaporthe grisea* (ATCC64557) and *Alternaria alternata* (MTCC2060) were procured from Institute of Microbial Technology (IMTECH), Chandigarh.

### 2.2. Preparation of leaf extract

Young leaves of *G. glauca* were confirmed by using herbarium specimens deposited at plants and animal museum, Karnatak University, Dharwad (Fig. 1). Leaves were cleaned a number of times and 20 g of leaves were weighed and diced into small pieces, which later transferred into sterile distilled water (250 mL) and agitated at 80 °C for 60 min on water bath for formation of aqueous leaf extract. This was sieved using Whatman No. 1 filter paper and filtrate was centrifuged at 5000 rpm for 5 min and the supernatant applied for synthesis of AgNPs.



Fig. 1. The plant *G. glauca*.

### 2.3. Bio-synthesis of AgNPs

One mM AgNO<sub>3</sub> solution was formulated by mixing 0.1698 g AgNO<sub>3</sub> in 1000 mL of distilled water and used for AgNPs synthesis. The prepared plant extract and AgNO<sub>3</sub> solutions were mixed in the ratio of 1:4 (v/v) in 1000 mL conical flask. The pH of reaction mixture was set at 8.5 and incubated in dark for 12 h. After the required incubation period the spectra was recorded with an UV-Vis. spectrophotometer. Finally, the mixture was centrifuged for 10 min at 10,000 rpm and acquired AgNPs were used for further analysis.

### 2.4. Characterizations of synthesized AgNPs

The Characterizations of synthesized AgNPs were performed according to the methods of Gaddala and Nataru, (2015), Fafal et al. (2017), Ghramh et al. (2020) and Sreenivasa et al. (2020). The spectrophotometric analysis was executed running a spectrophotometer (UV-9600A, METASH Instruments Co. Ltd., UV/Vis. spectrophotometer, Shanghai, China) in the array of 300 to 700 nm. The FTIR study was performed for leaf aqueous extract and AgNPs to decipher properties of compounds containing functional groups on surface of AgNPs with FTIR (NICOLET 6700, Thermo Fisher Scientific, Waltham, Massachusetts, USA) in the range of 400 to 4000 cm<sup>-1</sup>. AFM was used for the study of size, distribution, dispersion and aggregation of AgNPs. SEM analysis was carried out for examining the degree of aggregation and surface imaging of AgNPs. The chemical composition of AgNPs was also performed using an EDX analyzer conjoined with SEM (JSMIT500, In Touch Scope Scanning Electron Microscope). HR-TEM technique was adopted to visualize the size distribution and surface morphology of AgNPs utilizing a HR-TEM (Hitachi, Model: S-3400 N). The crystalline structure and size of AgNPs at atomic scale was investigated by XRD analysis [CuK $\alpha$  radiation ( $\lambda = 0.154$  nm) at 2 $\theta$  angles ranged from 30° to 80°] (Rigaku smartlab SE). Later, the particle size was calculated with Dubey Scherrer equation,  $D = 0.90\lambda/\beta\cos\theta$ . The thermal stability of AgNPs and its constituents was analyzed by TGA. The temperature ranged from 27 °C to 600 °C at scanning rate of 10 °C/min using a Thermo gravimetric analyzer (TA Instruments, SDT Q600, USA). Finally, the zeta potential of AgNPs was inspected by zeta analyzer instrument (Horiba scientific nanoparticle analyzer SZ-100).

### 2.5. In-vitro antioxidant activity (DPPH assay)

Free radical scavenging assay of DPPH was carried out to evaluate the antioxidant potential of *G. gluca* synthesized AgNPs. One mg of AgNPs was mixed in 1 mL of distilled water and from this; 100 to 1000  $\mu$ g/mL concentrations of AgNPs were prepared separately by mixing with water. DPPH solution (0.1 mM) was prepared with methanol and used as blank, whereas ascorbic acid was treated as positive control. Later, each concentration of AgNPs dispersion was combined with 3 mL DPPH solution and incubated in dark chamber and room temperature for 30 min. Further, the absorbance was determined at 517 nm. The percentage inhibition of radical scavenging was computed by following formula:

% of free radical scavenging activity

$$= \frac{(\text{Absorbance of control} - \text{Absorbance of test}) \times 100}{\text{Absorbance of control}}$$

### 2.6. Assessment of antimicrobial activity

Antibacterial activity was carried out through well diffusion method on Nutrient agar for bacteria and potato-dextrose agar

for fungi. The AgNPs concentration was formulated by completely mixing 1 mg AgNPs in 1 mL autoclaved distilled water. 100  $\mu$ L of each bacteria and fungi (0.5 McFarland concentrations) were swabbed on these media in separate plates and 6 mm wells were made. Each well for bacteria and fungi were filled with 100  $\mu$ L of positive control (streptomycin for bacteria and fluconazole for fungi) and negative control (autoclaved distilled water) and 25, 50 and 100  $\mu$ L of AgNPs suspension. After incubation the zone of inhibitions were measured and recorded.

### 2.7. In-Vitro anticancer activity

Human liver adenocarcinoma-SK-HEP1 cell line was purchased from NCCS, Pune and evaluated for *in-vitro* anticancer activity. An approximate number of cells (20000 cell/well in 200  $\mu$ L) were pipetted into 96 well plates and different concentrations of AgNPs (12.5, 25, 50, 100, 200  $\mu$ g/mL) was added and preceded by incubation at 37 °C for 24 h. Medium with cells mixed with 10  $\mu$ M of Camptothecin was determined as positive control and cells in medium without any experimental compound was termed as negative control. Then 200  $\mu$ L of MTT (5 mg/mL) reagent was added and incubated the plates for 3 h in same conditions. After the incubation, the MTT reagent was discarded and 100  $\mu$ L of DMSO was mixed as solubilisation solution. Finally the absorbance was measured on an ELISA reader at 570 nm and IC<sub>50</sub> value was calculated using linear regression equation.

### 2.8. Apoptotic assay of cancer cell line

Apoptotic study was conducted to determine the viability of SK-HEP1 cell line using Acridine orange (AO) and Ethidium Bromide (EtBr). The cancer cells were cultured in 6 well plates and treated with IC<sub>50</sub> concentration (19.12  $\mu$ g/mL) of AgNPs (average size 26 nm). The cells with no AgNPs treatment were termed as control. Later, the cells in all the 6 wells were stained with 200  $\mu$ L of AO and EtBr for 10 min and observed under fluorescence microscope using Image-J Software v1.48.

### 2.9. Statistical analysis

Statistical analysis was carried out using the software called SPSS. For calculations of standard deviation  $P \leq 0.05$  was found as statistically significant.

## 3. Results and discussions

The present investigation on synthesis of AgNPs applying aqueous leaf extract of *G. gluca* was affirmed by change in color of the reaction mixture from yellowish to brown after incubation in room temperature for 12 h at pH 8.5 (Fig. 2A and B). The alteration in the color roughly demonstrated the synthesis of AgNPs. It was reported that the color change may be due to the existence of co-enzyme NAD<sup>+</sup> or ascorbic acid found in living cells, which are involved in redox reaction and thereby transform Ag<sup>+</sup> ions in the reaction mixture to Ag<sup>0</sup> (zero-valence state) (Gaddala and Nataru, 2015). The pH 8.5 was found the most appropriate producing a UV-Vis. spectrum in 400–500 nm range for AgNPs synthesis (Murali et al., 1997). Similar phenomenon of color change to brown was also reported by Jalaluddin et al. (2016).

The UV-Vis. spectrum of *G. glauca* leaves extract was shown in (Fig. 2C). The formation of AgNPs using *G. glauca* leaves extract was endorsed by obtaining UV-Vis. spectrum at 402 nm (Fig. 2D). The maximum absorption spectrum at 402 nm confirmed the synthesis of AgNPs, which was due to excitation of SPR phenomenon of nanoparticles. The free electrons present on AgNPs are the reason

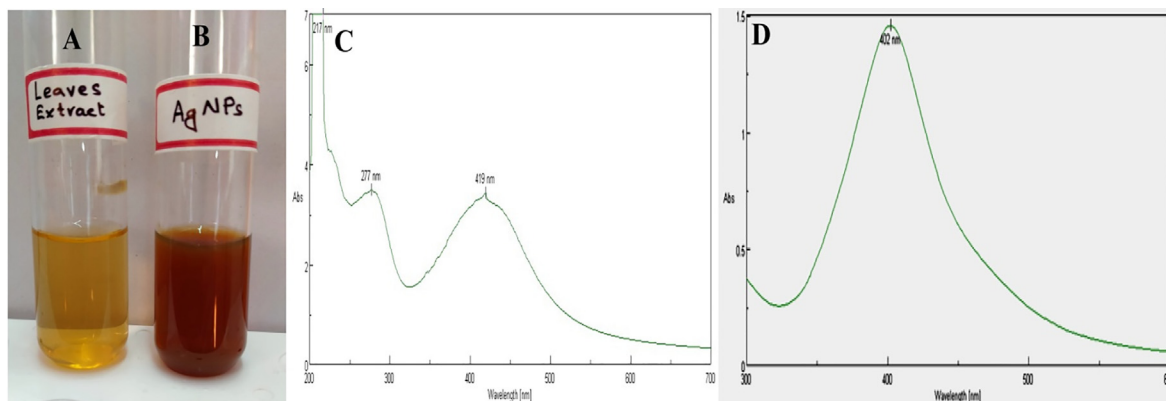


**Fig. 2.** Change in color of reaction mixture after mixing with  $\text{AgNO}_3$ . (A) Leaf aqueous extract, (B) Brown color indicated production of AgNPs and (C) UV-Vis. spectrum of *G. glauca* leaf extract and (D) UV-Vis. spectrum of synthesized AgNPs from *G. glauca* leaf extract.

of SPR and plays a crucial role on size of AgNPs (Mock et al., 2002). This observation was conceded with the results of Moodley et al. (2018).

The FTIR spectroscopic analysis was studied to detect compounds containing functional groups present in plant aqueous extract and subjected to reduce  $\text{Ag}^+$  ions and capping for AgNPs. The IR spectrum of *G. glauca* leaves extract revealed that there were marginal shifts in some peak positions of IR spectrum of AgNPs due to bioreduction detected in Fig. 3A and B respectively. The FTIR spectrum of leaves extract revealed strong spectral positions at 2978, 2372, 1647, 1462, 1086, 926, 860, 825 and 714  $\text{cm}^{-1}$ , whereas AgNPs displayed distinct peaks various functional groups at 2989, 2387, 1655, 1477, 1099, 930, 864, 829 and 717  $\text{cm}^{-1}$ . The distinct absorption bands at 2987 and 2989  $\text{cm}^{-1}$  appeared for C–H stretching of Alkanes. The peaks at 2372 and 2387  $\text{cm}^{-1}$  represented P–H stretching of phosphine and the bands at 1647 and 1655  $\text{cm}^{-1}$  indicated C = N stretching of imine or oxime. The region of 1462 and 1477  $\text{cm}^{-1}$  was a result of C–C stretching of aromatics. Peaks at 1086 and 1099  $\text{cm}^{-1}$  were appeared by virtue of C–O stretching of aliphatic ether and the peaks appeared at 926 and 930  $\text{cm}^{-1}$  were due to trans = C–H out of plane bending. The peaks in the region of 860 and 864  $\text{cm}^{-1}$  correlated to P–O–C stretch of aromatic phosphates, whereas bands at 825 and 829  $\text{cm}^{-1}$  indicated C = C bending of trisubstituted alkene as in the case of amino acids, proteins and flavonoids. Finally the bands at 714 and 717  $\text{cm}^{-1}$  represented C–Cl stretching of halo compounds. The shifts in the peaks of FTIR spectra indicated the involvement of functional groups of phytochemicals in biosynthesizing AgNPs. Leaf extract of *G. glauca* contains various phytochemicals, like fla-

vonoids, alkaloids, phenolics, tannins, saponins, anthraquinones, proteins and amino acids (Gupta and Jeevaratnam, 2018). This information indicated that the  $\text{Ag}^+$  ions might be reduced to  $\text{Ag}^0$  by carbonyl groups of flavonoids and free amino groups of proteins and subsequently capped and stabilized by other phytochemicals. An identical result was recorded by Fafal et al. (2017), where FTIR spectrum of *Asphodelus aestivus* plant mediated synthesis of AgNPs denoted the availability of biomolecules liable to capping and reducing.

The AFM is a spectroscopic method used to investigate the topology, size, shape, dispersion and agglomeration of AgNPs with the aid of a probe tip at atomic scale. The two-dimensional (2D) image of AgNPs showed the nanoparticles were poly-dispersed with a spherical shape having particles size 19 to 37 nm (Fig. 4A). The Fig. 4B and 4C revealed the distribution and histogram of AgNPs respectively. A result was achieved by Nayaka et al. (2020), where AFM measurement of synthesized AgNPs was in 25 to 75 nm ranges.

SEM micrograph displayed the AgNPs were spherical or oval shaped along with few polymorphic particles (Fig. 4D). The particles were poly-dispersed and few were agglomerated with a size ranged from 20 to 45 nm. A similar result was obtained by Kumar et al. (2016), where the SEM result of *Adansonia digitata* fruit synthesized AgNPs revealed the spherical and poly-dispersed nanoparticles having size between 18 and 32 nm.

The EDS spectrum of AgNPs showed different peaks. However, the distinct absorption peaks at 3 KeV were owing to presence of metallic silver in nanoparticles (Fig. 4E). These peaks are associated with characteristic binding energies like AgL $\alpha$ , AgL $\beta$  and AgL $\beta$ 2. The

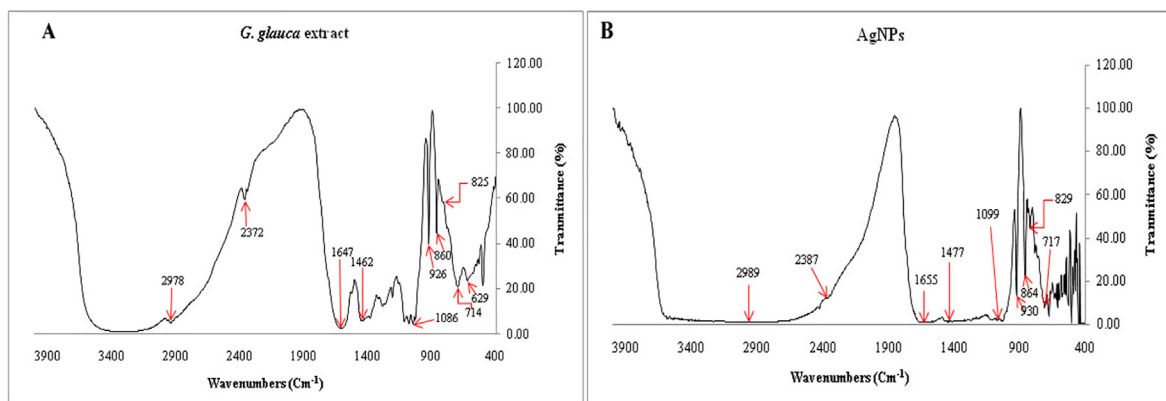


**Fig. 3.** FTIR spectra of *G. glauca* leaf extract and AgNPs. (A) *G. glauca* leaf extract and (B) AgNPs.

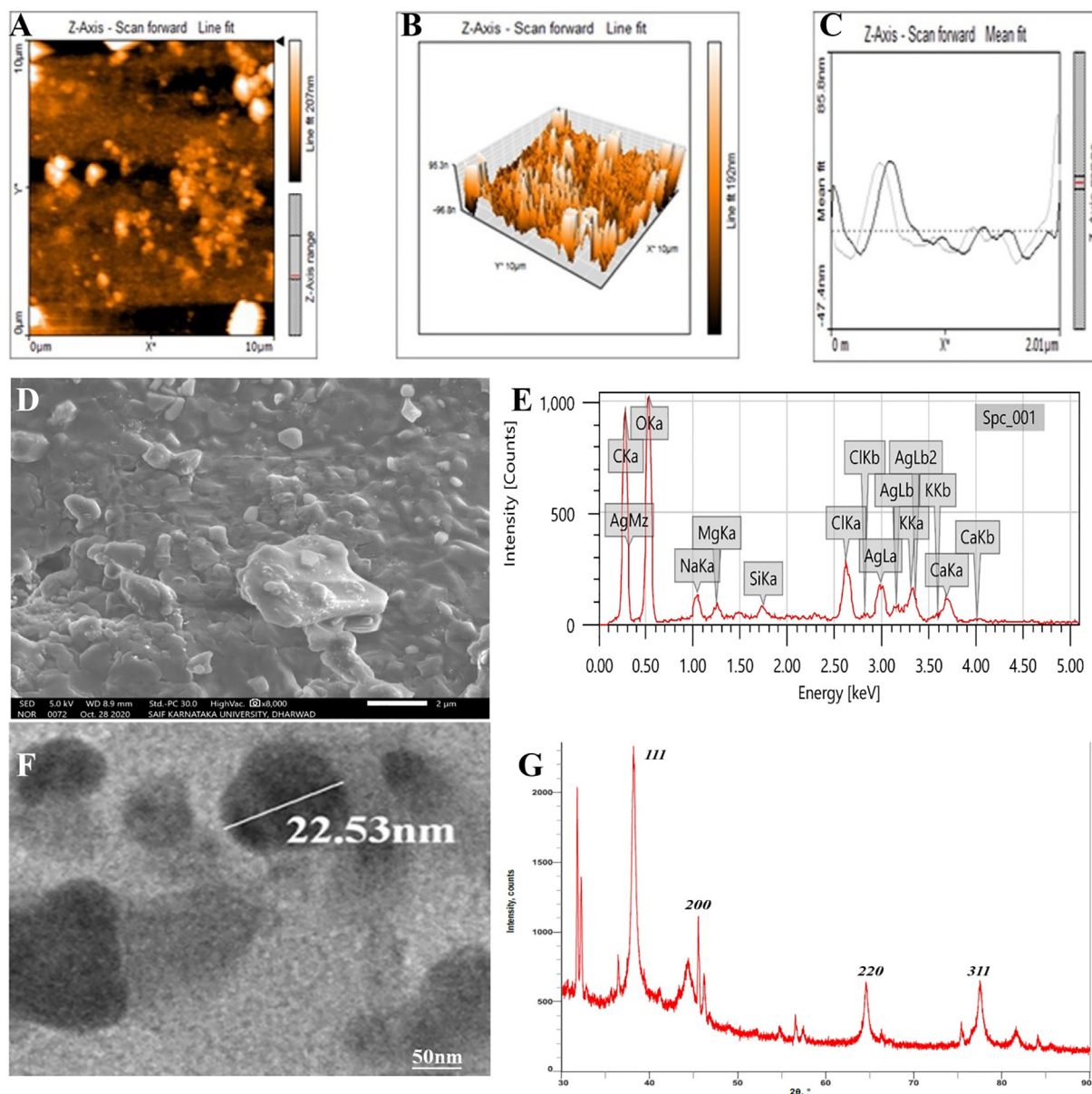


**Fig. 4.** (A) AFM 2D image, (B) AFM 3D image, (C) AFM Particles size distribution, (D) SEM analysis, (E) EDS spectrum, (F) TEM micrograph and (G) XRD spectrum.

other peaks present in the spectrum were in accordance with carbon, oxygen, sodium, magnesium, chlorine, calcium, etc. This result was consistent with earlier reports of Chand et al. (2020).

HR-TEM is a frequently used and valuable micro-imaging technique to access quantitative measures of nanoparticle size, shape, morphology and distribution of nanoparticles. HR-TEM images manifested spherical to oval shaped AgNPs as shown in Fig. 4F. All the particles were poly-dispersed having size ranged between 17 and 40 nm with an average size 27.30 nm. This was confirmative with the result of Rautela et al. (2019), where TEM images of *Tectona grandis* seed mediated AgNPs demonstrated spherical nanoparticles within 10 to 30 nm ranges.

The XRD spectrum indicated the crystalline nature and size of synthesized AgNPs. Four distinct diffraction peaks of  $2\theta$  angles were recorded at  $38.15^\circ$ ,  $44.28^\circ$ ,  $64.50^\circ$  and  $77.45^\circ$  and coordinated with JCPDS database of silver (file No. 04-0783) (Fig. 4G). These could be indexed at (1 1 1), (2 0 0), (2 2 0) and (3 1 1) Bragg's reflection of face centred cubic crystalline structure of AgNPs respec-

tively. The average size of AgNPs was calculated approximately 26 nm using Debye-Scherrer equation. In addition to this there were few other distinct peaks in the XRD spectrum at  $31.77^\circ$ ,  $32.21^\circ$ ,  $45.51^\circ$ ,  $56.54^\circ$ . The presence of these peaks might be due to the phyto-constituents or  $\text{AgNO}_3$ , which might have not been reduced and hence gave rise to these peaks (Rautela et al., 2019; Nayaka et al., 2020). This result could be confirmed with the result of Du et al. (2016).

The thermal gravimetric curve of AgNPs was depicted in Fig. 5A. The primary step of decomposition of AgNPs occurred between 57 and  $179^\circ\text{C}$ . There was a weight loss of 7.64%; this was probably due to evaporation of moisture from surface of AgNPs. In next step the temperature was increased from 179 to  $253^\circ\text{C}$  and associated with a loss of weight of 9.7%. In a further degradation, there was steady increase in temperature from 253 to  $297^\circ\text{C}$  resulted the weight loss of about 29%, which was mostly due to degenerated organic biomolecules, such as flavonoids, carbohydrates, proteins, phenolics, etc. present on the periphery of AgNPs. Further, the temperature was increased from 297 to  $478^\circ\text{C}$  leading to a weight loss of

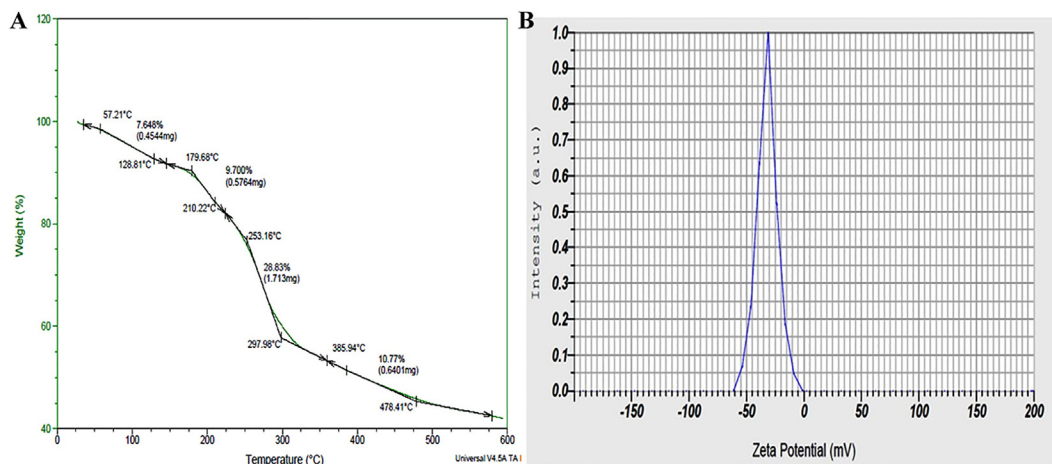


Fig. 5. (A) TGA curve, (B) Zeta potential of bio-synthesized AgNPs from *G. glauca* leaf extract.

11%; this could probably be assigned to thermal decomposition of resistant aromatic biomolecules present on the surface of AgNPs. This TGA curve implies the stability of *G. glauca* synthesized AgNPs even at higher temperature up to 180 °C and even provides the evidence that the AgNPs were covered with the bioactive organic compounds from *G. glauca* leaf extract (Luminita and Bianca, 2020). This obtained result can be compared with the findings of Okaiyeto et al. (2021).

The zeta potential is an index of surface charge potential and a significant parameter to understand the nanoparticles stability in aqueous suspension. The zeta potential of AgNPs was found as a sharpened peak at  $-32.0 \pm 0.5$  mV (Fig. 5B) and indicated a significant stability the AgNPs. Owing to the negative value of zeta potential the nanoparticles were poly-dispersed, indicating their long term stability in the suspension. The electrostatic repulsive force among each other resulted in prevention of aggregation of the nanoparticles. This result was comparable with the result Erdogan et al. (2019), where the Zeta potential of AgNPs was estimated  $-32.3 \pm 0.8$  mV.

### 3.1. In-vitro antioxidant activity (DPPH assay)

Antioxidants are also known as free radical scavengers and help prevent and control damages and reduce the risks of other degenerative ailments caused by reactive oxygen species (ROS) (Singh

et al., 2018). The DPPH radical scavenging action of bio-synthesized AgNPs and *G. glauca* extract was depicted in Fig. 6. Scavenging activity of *G. glauca* AgNPs was detected in various concentrations from 100, 200, 400, 600, 800 and 1000 µg/mL, where the inhibition ratio were  $48.75 \pm 1.14\%$ ,  $53.48 \pm 1.76\%$ ,  $59.19 \pm 2.45\%$ ,  $67.05 \pm 1.11\%$ ,  $74.1 \pm 1.47\%$  and  $77.67 \pm 1.36\%$  respectively. The AgNPs implies a significant increase in scavenging potency in a dose dependent way by transferring electrons to terminate the free radicals in DPPH although the activity was lesser than ascorbic acid (positive control). The *G. glauca* leaf extract alone expressed the lowest antioxidant activity against DPPH free radicals. Phenolics and flavonoids are the most important phytochemicals known to have good antioxidant potential. Therefore it can be assumed that AgNPs may have been capped with more phenolic and flavonoid compounds and resulted in a significant antioxidant activity (Singh et al., 2018; Saumya and Basha, 2011). This result was confirmed with the result of *Cucumis prophetarum* leaf extract synthesized AgNPs (Hemlata et al., 2020).

### 3.2. Antimicrobial activity

The antimicrobial study revealed a powerful activity against all pathogenic bacteria and fungi. Antimicrobial activity of AgNPs was depicted in Fig. 7A to J. The Fig. 7K indicated the inhibition zones for different concentrations of AgNPs and positive controls. This

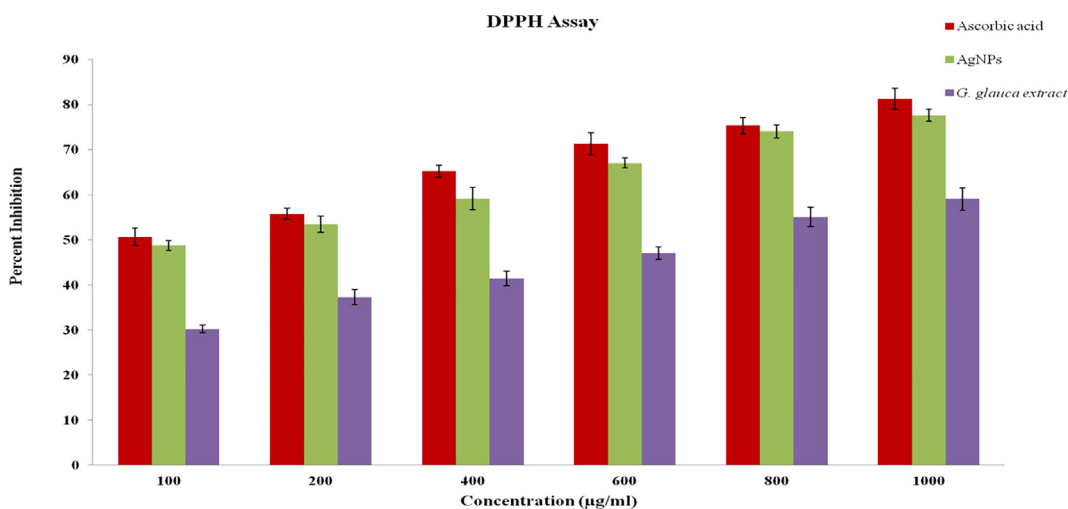
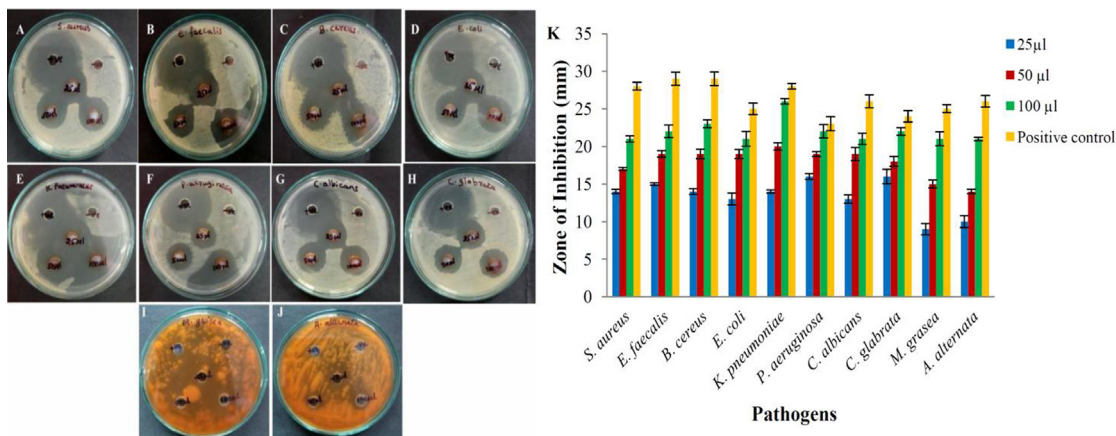


Fig. 6. DPPH radical scavenging assay of *G. glauca* synthesized AgNPs.



**Fig. 7.** Antimicrobial activity *G. glauca* synthesized AgNPs. (A) *S. aureus*, (B) *E. faecalis*, (C) *B. cereus*, (D) *E. coli*, (E) *K. pneumoniae*, (F) *P. aeruginosa*, (G) *C. albicans*, (H) *C. glabrata*, (I) *M. grisea*, (J) *A. alternata* and (K) Graph of zone of inhibition of AgNPs.

result deciphered the inhibitory action was gradually raised along the increasing concentrations of AgNPs. The Fig. 7K implicid that *P. aeruginosa* and *C. glabrata* were most susceptible and *M. grasea* and *A. alternata* were least susceptible to the lowest concentration of AgNPs (25 µL). This considerable antimicrobial activity was due to the ratio of large surface area to volume of AgNPs, which establish a better association with pathogens. It was even noted the nanoparticles easily attract the microorganisms due to their small size and the electrostatic traction between less negatively or positively charged AgNPs and negatively charged microbial cell membrane and pass through the cell wall (Abbaszadegan et al., 2015).

Upon penetration into cell wall the AgNPs lead to morphological deformities in membrane architecture and cause depletion of ATP via disruption of respiratory functions, which conclusively lead to cell death (Nayaka et al., 2020; Roy et al., 2019).

### 3.3. In-vitro anticancer activity

The bio-synthesized AgNPs exhibited direct dose dependent cytotoxic potential towards SK-HEP1 cells as shown in Fig. 8. The negative and positive controls were shown in Fig. 8A and 8B respectively. The cytotoxicity was gradually enhanced along

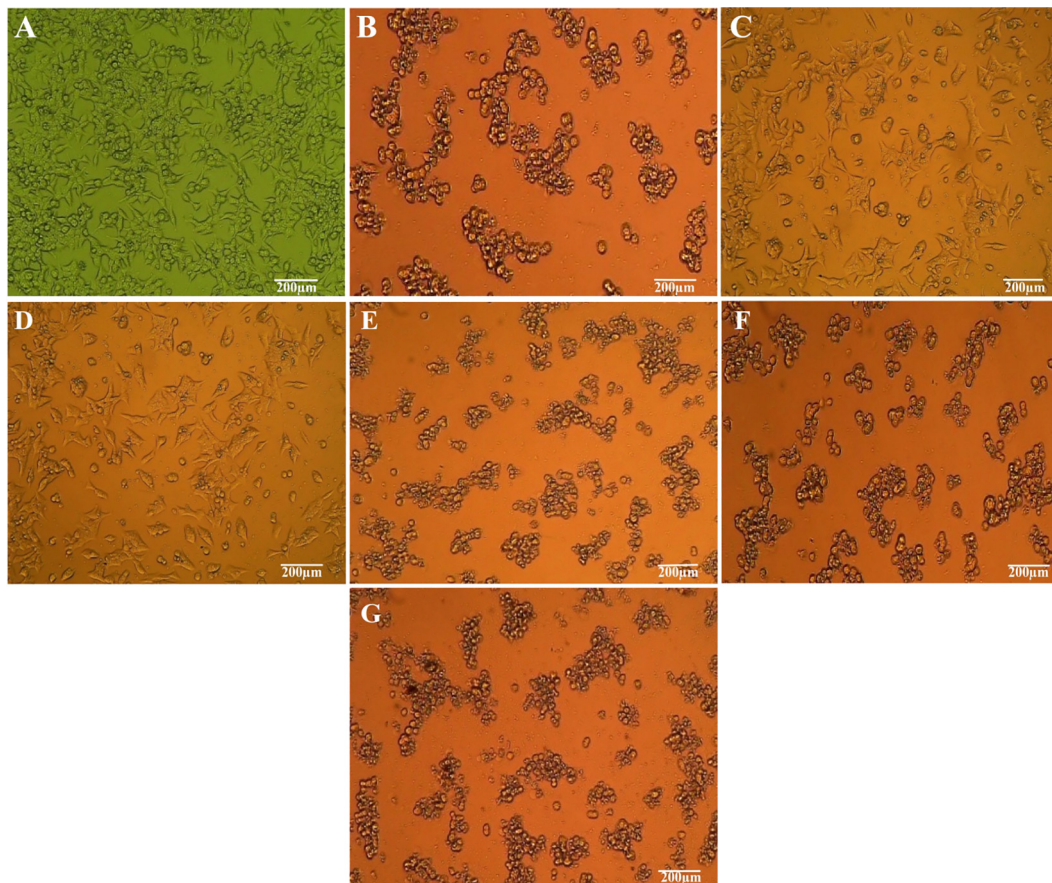


**Fig. 8.** Anticancer assay of different concentration of bio-synthesized AgNPs. (A) Negative control, (B) Positive control, (C) 12.5 µg/mL, (D) 25 µg/mL, (E) 50 µg/mL, (F) 100 µg/mL, (G) 200 µg/mL.

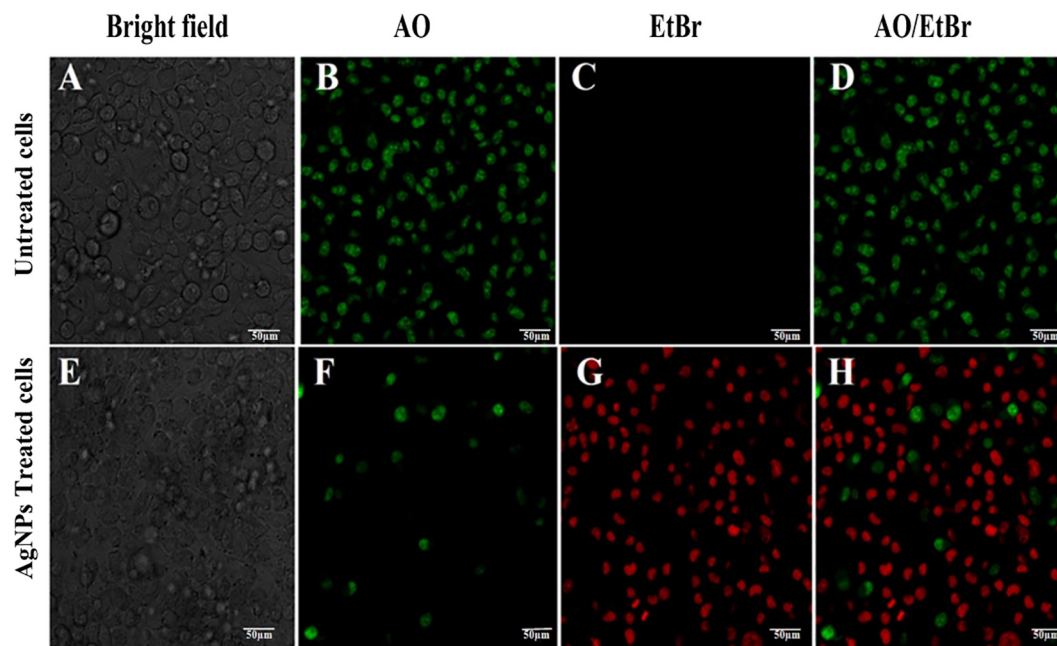


**Fig. 9.** Apoptotic study of AgNPs against SK-HEP1 cell line; (A) Untreated cells, (B) Untreated cells stained with AO, (C) Untreated cells with EtBr, (D) Untreated cells stained with AO and EtBr, (E) Cells treated with  $IC_{50}$  conc. of AgNPs, (F) Treated cells stained with AO, (G) Treated cells stained with EtBr and (H) Treated cells stained with AO and EtBr.

gradual rising concentration of AgNPs from 12.5  $\mu\text{g}/\text{mL}$  to 200  $\mu\text{g}/\text{mL}$  (Fig. 8C to G). The viability of cancer cells was 50.29% at 12.5  $\mu\text{g}/\text{mL}$  AgNPs and it was reduced to a viability of 3.71% during the treatment with 200  $\mu\text{g}/\text{mL}$  AgNPs. The  $IC_{50}$  value was calculated to be 19.12  $\mu\text{g}/\text{mL}$ . This result could be compared to the result of Sabah et al. (2020), where *B. oleracea* leaf synthesized AgNPs expressed anticancer activity at an  $IC_{50}$  value of 55  $\mu\text{g}/\text{mL}$ . AgNPs are known to be anticancerous through different probable mechanisms however; the proper reaction of AgNPs on cancer cells is still unrecognized. It was reported that the AgNPs released  $\text{Ag}^+$  ions, which has a strong attraction to membrane proteins of cancer cells. These  $\text{Ag}^+$  ions later interact with nucleic acids like RNA and DNA damage and induce chromosomal aberrations (Preethi et al., 2006; Sreenivasa et al., 2020). The AgNPs was even noted as genotoxic and mutagenic due to presence of flavonoids and alkaloids on their surface (Ghramh et al., 2020).

### 3.4. Apoptotic assay

The AO/EtBr staining is a quantitative and qualitative method to find out apoptosis in tumor cells. In this experiment the control cells emitted green fluorescence by staining with AO and indicated viable cells and apoptotic cells were stained red with EtBr (Fig. 9). However, only few viable were found in AgNPs treated cancer cells. The red fluorescence was emitted by most of the cells, indicated the late apoptotic or dead cells. The figure revealed  $IC_{50}$  concentration of AgNPs able to produce an impressive cytotoxicity to SK-HEP1 cell line. The results were compared with Roy et al. (2019), where the effect of alpha linolenic acid on MCF-7 cancer cell lines was examined through Apoptotic assay by AO/EtBr staining.

## 4. Conclusions

In this study an eco-friendly, cost effective bio-synthesis of AgNPs was accomplished using *G. glauca* aqueous leaf extract. The UV spectra demonstrated a peak at 402 nm and particle size was 17 to 40 nm. The FTIR spectra demonstrated phytochemicals, such as flavonoids, phenolics, proteins mainly responsible for

AgNPs synthesis and a long term stability of AgNPs was analyzed by zeta potential analysis investigation. The bio-synthesized AgNPs exhibited a significant antioxidant activity and therefore it might be useful in treating various incurable diseases. Antimicrobial assay of AgNPs exhibited a potential inhibitory activity of pathogenic organisms, thus it may lead a way in advancement of treating bacterial and fungal diseases. Finally, the AgNPs revealed an efficient anticancer activity against SK-HEP1 cell line. Hence, it was suggested the *G. glauca* synthesized AgNPs could be used in treatment of liver cancer after further in-vivo experiments. Therefore, future investigations are required to fully understand the mechanism and extensive in-vivo characterization of antioxidant, antibacterial and anticancer efficiency associated with the particles.

### Declaration of Competing Interest

The authors declare that they have no known competing financial interests or personal relationships that could have appeared to influence the work reported in this paper.

### Acknowledgement

The authors of the research work greatly acknowledge the P.G. Department of Studies in Botany, Karnatak University, Dharwad for extending lab facilities. The authors are even thankful to University Scientific Instrumentation Centre (USIC), Karnatak University, Dharwad for essential instrumentation services. This project was supported by seed grant for research program (2021-22/62), Karnatak University, Dharwad, Karnataka, India. This project was supported by Researchers Supporting Project number (RSP-2021/142), King Saud University, Riyadh, Saudi Arabia.

### References

- Abbaszadegan, A., Ghahramani, Y., Gholami, A., Hemmateenejad, B., Dorostkar, S., Nabavizadeh, M., Sharghi, H., 2015. The effect of charge at the surface of silver nanoparticles on antimicrobial activity against gram-positive and gram-



- negative bacteria: a preliminary study. *J. Nanomater.* 2015. <https://doi.org/10.1155/2015/720654> 720654.
- Abou El-Nour, K.M.M., Eftaiha, A., Al-Warthan, A., Ammar, R.A.A., 2010. Synthesis and applications of silver nanoparticles. *Arab. J. Chem.* 3 (3), 135–140. <https://doi.org/10.1016/j.arabjc.2010.04.008>.
- Anderson, C., 2007. Revision of *Galphimia* (*Malpigiaceae*). *Contr. Univ. Michigan. Herb.* 25, 1–82.
- Awad, A.M., Salem, N.M., Abdeen, A.O., 2013. Green synthesis of silver nanoparticles using carob leaf extract and its antibacterial activity. *Int. J. Ind. Chem.* 4, 29. <https://doi.org/10.1186/2228-5547-4-29>.
- Cardoso-Taketa, A.T., Pereda-Miranda, R., Choi, Y.H., Verpoorte, R., Villarreal, M.L., 2008. Metabolic profiling of the Mexican anxiolytic and sedative plant *Galphimia glauca* using nuclear magnetic resonance spectroscopy and multivariate data analysis. *Planta Med.* 74 (10), 1295–1301. <https://doi.org/10.1055/s-2008-1074583>.
- Chand, K., Cao, D., Eldin, D., Hussain, A., Qadeer, A., Zhu, K., Nazim, M., Mehdi, G., 2020. Green synthesis, characterization and photocatalytic application of silver nanoparticles synthesized by various plants extracts. *Arab. J. Chem.* 13 (11), 8248–8261. <https://doi.org/10.1016/j.arabjc.2020.01.009>.
- Das, R.K., Laxman, V., Linson, P., 2017. Biological synthesis of metallic nanoparticles: plants, animals and microbial aspects. *Nanotechnol. Environ. Eng.* 2, 18. <https://doi.org/10.1007/s41204-017-0029-4>.
- Devanesan, S., AlSalhi, M.S., 2021. Green synthesis of silver nanoparticles using the flower extract of *Abelmoschus esculentus* for cytotoxicity and antimicrobial studies. *Int. J. Nanomed.* 16, 3343–3356. <https://doi.org/10.2147/IJN.S307676>.
- Devanesan, S., Jayamala, M., AlSalhi, M.S., Umamaheshwari, S., Ranjitsingh, A.J.A., 2021. Antimicrobial and anticancer properties of *Carica papaya* leaves derived di-methyl flubendazole mediated silver nanoparticles. *J. Infect. Public Health* 14 (5), 577–587. <https://doi.org/10.1016/j.jiph.2021.02.004>.
- Du, J., Singh, H., Yi, T.-H., 2016. Antibacterial, anti-biofilm and anticancer potentials of green synthesized silver nanoparticles using benzoin gum (*Styrax benzoin*) extract. *Bioprocess Biosyst. Eng.* 39 (12), 1923–1931. <https://doi.org/10.1007/s00449-016-1666-x>.
- Erdogan, O., Abbak, M., Demirbolat, G.M., Birtokocak, F., Aksel, M., Pasa, S., Cevik, O., Mukherjee, A., 2019. Green synthesis of silver nanoparticles via *Cynara scolymus* leaf extracts: The characterization, anticancer potential with photodynamic therapy in MCF7 cells. *PLoS One* 14 (6), e0216496. <https://doi.org/10.1371/journal.pone.0216496>.
- Fafal, T., Taştan, P., Tuzun, B.S., Ozyazici, M., Kivcak, B., 2017. Synthesis, characterization and studies on antioxidant activity of silver nanoparticles using *Asphodelus aestivus* Brot. aerial part extract. *South African J. Bot.* 112, 346–353. <https://doi.org/10.1016/j.sajb.2017.06.019>.
- Gaddala, B., Nataru, S., 2015. Synthesis, characterization and evaluation of silver nanoparticles through leaves of *Abrus precatorius* L.: an important medicinal plant. *Appl. Nanosci.* 5 (1), 99–104. <https://doi.org/10.1007/s13204-014-0295-4>.
- Ghramh, H.A., Ibrahim, E.H., Kilnay, M., Ahmad, Z., Alhag, S.K., Khan, K.A., Taha, R., Asiri, F.M., 2020. Silver nanoparticle production by *Ruta graveolens* and testing its safety, bioactivity, immune modulation, anticancer, and insecticidal potentials. *Bioinorg. Chem. Appl.* 2020, 1–11. <https://doi.org/10.1155/2020/5626382>.
- Gupta, R., Jeevaratnam, K., 2019. A comparative evaluation of in vitro phytochemical analysis, antioxidant, antibacterial and anticancer activity of methanolic (MeOH) crude extract of bark (GGB) and leaf (GGL) of *Galphimia glauca*. *Int. J. Emerg. Technol. Innov. Res.* 6, 830–842.
- Gurunathan, S., Han, J.W., Park, J.H., Kim, J.H., 2014. A green chemistry approach for synthesizing biocompatible gold nanoparticles. *Nanoscale Res. Lett.* 9, 248. <https://doi.org/10.1186/1556-276X-9-248>.
- Guzel, R., Erdal, G., 2018. Synthesis of silver nanoparticles, in: Maaz K. (Eds.), *Silver Nanoparticles: Fabrication, Characterization and Applications*, IntechOpen, pp. 1–20. <https://doi.org/10.5772/intechopen.75363>.
- Hemlata, Meena, P.R., Singh, A.P., Tejavath, K.K., 2020. Biosynthesis of silver nanoparticles using *Cucumis prophetarum* aqueous leaf extract and their antibacterial and antiproliferative activity against cancer cell lines. *ACS Omega* 5 (10), 5520–5528. <https://doi.org/10.1021/acsomega.0c00155>.
- Jalaluddin, M.A., Mohammad, A.A., Haris, M.K., Mohammad, A.A., Inho, C., 2016. Green synthesis of silver nanoparticles and characterization of their inhibitory effects on AGEs formation using biophysical techniques. Green synthesis of silver nanoparticles and characterization of their inhibitory effects on AGEs formation using biophysical techniques. *Sci. Rep.* 6, 20414. <https://doi.org/10.1038/srep20414>.
- Kumar, C.M.K., Yugandhar, P., Savithamma, N., 2016. Biological synthesis of silver nanoparticles from *Adansonia digitata* L. fruit pulp extract, characterization, and its antimicrobial properties. *J. Interact. Ethnopharmacol.* 5 (1), 79–85. <https://doi.org/10.5455/jice.20160124113632>.
- Luminita, D., Bianca, M., 2020. Green Synthesis of Biogenic Silver Nanoparticles for Efficient Catalytic Removal of Harmful Organic Dyes, *Nanomaterials* 10(2), 202. <https://doi.org/10.3390/nano10020202>.
- Mock, J.J., Barbic, M., Smith, D.R., Schultz, D.A., Schultz, S., 2002. Shape effects in plasmon resonance of individual colloidal silver nanoparticles. *J. Chem. Phys.* 116 (15), 6755–6759. <https://doi.org/10.1063/1.1462610>.
- Moodley, J.S., Krishna, S.B.N., Pillay, K., Sershen, G.P., 2018. Green synthesis of silver nanoparticles from *Moringa oleifera* leaf extracts and its antimicrobial potential. *Adv. Nat. Sci. Nanosci. Nanotechnol.* 9 (1), 015011. <https://doi.org/10.1088/2043-6254/aaabb2>.
- Murali, S., Mayya, K.S., Bandyopadhyay, K., 1997. pH Dependent changes in the optical properties of carboxylic acid derivatized silver colloidal particles 127 (1–3), 221–228. [https://doi.org/10.1016/S0927-7757\(97\)00087-3](https://doi.org/10.1016/S0927-7757(97)00087-3).
- Nayaka, S., Bidhayak, C., Bhat, M.P., Nagaraja, S.K., Airodagi, D., Swamy, P.S., Rudrappa, M., Hiremath, H., Basavarajappa, D.S., Kanakannavar, B., 2020. Biosynthesis, characterization, and in vitro assessment on cytotoxicity of actinomycete-synthesized silver nanoparticles on *Allium cepa* root tip cells. *Beni-Suef Univ. J. Basic Appl. Sci.* 9, 51. <https://doi.org/10.1186/s43088-020-00074-8>.
- Okaiyeto, K., Hoppe, H., Okoh, A.I., 2021. Plant-based synthesis of silver nanoparticles using aqueous leaf extract of *Salvia officinalis*: characterization and its antiparasitoid activity. *J. Clust. Sci.* 32 (1), 101–109. <https://doi.org/10.1007/s10876-020-01766-y>.
- Oza, G., Calzadilla-Avila, A.I., Reyes-Calderón, A., Anna, K.K., Ramírez-Bon, R., Tapia-Ramirez, J., Sharma, A., 2020. pH-dependent biosynthesis of copper oxide nanoparticles using *Galphimia glauca* for their cytocompatibility evaluation. *Appl. Nanosci.* 10 (2), 541–550. <https://doi.org/10.1007/s13204-019-01159-2>.
- Ponarulseelvam, S., Panneseelvam, C., Murugan, K., Aarthi, N., Kalimuthu, K., Thangamani, S., 2012. Synthesis of silver nanoparticles using leaves of *Catharanthus roseus* Linn. G. Don and their antiparasitoid activities. *Asian Pac. J. Trop. Biomed.* 2(7), 574–580. [https://doi.org/10.1016/S2221-1691\(12\)60100-2](https://doi.org/10.1016/S2221-1691(12)60100-2).
- Preethi, K.C., Kuttan, G., Kuttan, R., 2006. Anti-tumour activity of *Ruta graveolens* extract. *Asian Pac. J. Cancer Prev.* 7(3), 439–443. 2006.
- Rautela, A., Rani, J., Debnath, (Das), M., 2019. Green synthesis of silver nanoparticles from *Tectona grandis* seeds extract: characterization and mechanism of antimicrobial action on different microorganisms. *J. Anal. Sci. Technol.* 10, 5. <https://doi.org/10.1186/s40543-018-0163-z>.
- Roy, A., Bulut, O., Some, S., Mandal, A.K., Yilmaz, M.D., 2019. Green synthesis of silver nanoparticles: biomolecule-nanoparticle organizations targeting antimicrobial activity. *RSC Adv.* 9 (5), 2673–2702. <https://doi.org/10.1039/C8RA08982E>.
- Sabah, A., Hajera, T., Norah, S.M.A., Mir, N.A., Basmah, A., Salma, A., Manal, A.N.B., Roua, A., 2020. Eco friendly silver nanoparticles synthesis by *Brassica oleracea* and its antibacterial, anticancer and antioxidant properties. *Sci. Rep.* 10, 18564. <https://doi.org/10.1038/s41598-020-74371-8>.
- Saumya, S., Basha, P., 2011. Antioxidant effect of *Lagerstroemia speciosa* Pers (Banaba) leaf extract in streptozotocin-induced diabetic mice. *Indian J. Exp. Biol.* 49, 125–131.
- Sharma, A., Angulo-Bejarano, P.I., Madariaga-Navarrete, A., Oza, G., Iqbal, H.M.N., Cardoso-Taketa, A., Villarreal, M.L., 2018. Multidisciplinary investigations on *Galphimia glauca*: a Mexican medicinal plant with pharmacological potential. *Molecules* 23 (11), 2985. <https://doi.org/10.3390/molecules23112985>.
- Singh, H., Du, J., Singh, P., Yi, T.H., 2018. Role of green silver nanoparticles synthesized from *Symphytum officinale* leaf extract in protection against UVB-induced photoaging. *J. Nanostruct. Chem.* 8 (3), 359–368. <https://doi.org/10.1007/s40097-018-0281-6>.
- Singh, P., Kim, Y.J., Zhang, D., Yang, D.C., 2016. Biological synthesis of nanoparticles from plants and microorganisms. *Trends. Biotechnol.* 34 (7), 588–599. <https://doi.org/10.1016/j.tibtech.2016.02.006>.
- Song, J.Y., Kim, B.S., 2009. Rapid biological synthesis of silver nanoparticles using plant leaf extracts. *Bioprocess Biosyst. Eng.* 32 (1), 79–84. <https://doi.org/10.1007/s00449-008-0224-6>.
- Sreenivasa, N., Bidhayak, C., Pallavi, S.S., Bhat, M.P., Shashiraj, K.N., Ghasti, B., 2020. Synthesis of biogenic silver nanoparticles using *Zanthoxylum rhetsa* (Roxb.) dc seed coat extract as reducing agent and in-vitro assessment of anticancer effect on a549 lung cancer cell line. *Int. J. Pharm. Res.* 12, 302–314. <https://doi.org/10.31838/ijpr.2020.12.03.024>.
- Veerasamy, R., Xin, T.Z., Gunasagar, S., Xiang, T.F.W., Yang, E.F.C., Jeyakumar, N., Dhanaraj, S.A., 2011. Biosynthesis of silver nanoparticles using mangosteen leaf extract and evaluation of their antimicrobial activities. *J. Saudi Chem. Soc.* 15 (2), 113–120. <https://doi.org/10.1016/j.jscs.2010.06.004>.
- Zhang, X.F., Liu, Z.G., Shen, W., Gurunathan, S., 2016. Silver nanoparticles: synthesis, characterization, properties, applications, and therapeutic approaches. *Int. J. Mol. Sci.* 17 (9), 1534. <https://doi.org/10.3390/ijms17091534>.